Caspian Journal of Environmental Sciences
Online ISSN: 1735-3866
Print ISSN: 1735-3033

Inhibition activity of aluminium oxide nanoparticles for herpes simplex type 1

Abbas. K. Almansorri[1], Hider. M. H. Al-Shirifi[2], Sharafaldin Al-Musawi[3*], Bara B Ahmed[1]

1. Faculty of Biotechnology, Al-Qasim Green University, Babylon, Iraq
2. Al-Qasim Green University, Environmental Sciences College, Environmental Health Department
3. College of Food Sciences, Al-Qasim Green University, Babylon Province, Iraq

** Corresponding author's E-mail: dr.sharaf@biotech.uoqasim.edu.iq*

ABSTRACT

Several studies have shown that herpes simplex type 1(HSV-1) is one of the viruses resistant to medications, so potential antiherpetic agents need to be evaluated. This study aimed to evaluate the impact of aluminium oxide Nanoparticles (Al_2O_3-NPs) on the HSV-1 infection. Characterization of Al_2O_3-NPs were performed using field emission scanning electron microscopy (FESEM), X-ray diffraction (XRD), dynamic light scattering (DLS), and high-resolution transmission electron microscopy (HRTEM). The MTT test was used to investigate the toxicity action of Al_2O_3-NPs on viable cells. Quantitative Real-Time PCR (qRT-PCR) and TCID50 assays were used to achieve antiherpetic performance of Al_2O_3-NPs. Indirect immunofluorescence assay (IFA) was performed to determine the inhibitory impact of Al_2O_3-NPs on viral antigen expression, and Acyclovir was utilized as a standard agent in all tests. HSV-1 was subjected to Al_2O_3-NPs at the maximum non-toxic concentration (100 µg mL^{-1}) led to a decrease of 0.1, 0.7, 1.8, and 2.5 log_{10} $TCID_{50}$ in the infectious titer relative to virus control ($P < 0.0001$). This concentration of Al_2O_3-NPs was correlated with 16.9%, 47.1 %, 61.2 %, 72.5 % and 74.6 % inhibition rate, calculated on the basis of HSV-1 viral load compared to virus control. Our results have shown that Al_2O_3-NPs exhibit a robust antiviral activity against HSV-1. This function demonstrates excellent potential for using Al_2O_3-NP in topical formulations for treating orolabial or genital herpetic lesions.

Keywords: Herpes Simplex Virus type 1, Aluminium oxide nanoparticles, Real-Time PCR, Antiviral Activity, Indirect immunofluorescence assay.
Article type: Research Article.

INTRODUCTION

Herpes simplex type 1 (HSV-1) is a highly infectious virus that is widespread and endemic worldwide. HSV-1 possesses double-stranded DNA and subcatagored in Herpesviridae and causes infections in the mouth more generally, transmitted through direct contact with body fluids or individual infected lesions (Zhang *et al.* 2017; James *et al.* 2014). HSV-1 displays many clinical effects, such as orolabial abnormalities, peripheral nervous system disorders, encephalitis, facial abnormalities and corneal blindness (Duarte *et al.* 2019). Both HSV-1 and HSV-2 are chronic diseases. Approximately 3.7 billion people under the age of 50 (67%) are globally infected with HSV-1. An approximately 491 million people worldwide aged 15-49 (13%) are infected with HSV-2 (https://www.who.int/news-room/fact-sheets/detail/herpes-simplex-virus) Antiviral drugs such as acyclovir, valacyclovir, and famciclovir are frequently the most drug treatments available for people with HSV infection. This antiviral drug is a deoxyguanosine analogue that generates its activity through inhibition of DNA polymerase enzyme of HSV-1 (Trigilio *et al.* 2012). There is increasing evidence for the development of HSV-1 resistant strains, that have formed a hindrance to the appropriate treating of their infections (Priengprom *et al.* 2015; Kongyingyoes *et al.* 2016). Besides, there are numerous studies on the adverse side effects of these drugs, like abdominal pain, nausea, vomiting, and neurotoxicity skin rashes, and diarrhoea (Morfin & Thouvenot 2003;

Caspian Journal of Environmental Sciences, Vol. 21 No. 1 pp. 125-133 Received: April 06, 2022 Revised: Aug. 18, 2022 Accepted: Sep. 03, 2022
DOI: 10.22124/CJES.2023.6203

Publisher: University of Guilan, Iran

Kakiuchi *et al.* 2017): As a result, there is a rising need to develop and investigate new therapeutic agents for HSV-1 that have a different mechanism of action than traditional medications. NPs offer unique physical properties and have been developed to treat infectious diseases (Al Musawi *et al.* 2019; Albukhaty *et al.* 2020; Suhad *et al.* 2021; Haider & Hussein 2022; Falih *et al.* 2022). These are primarily attributed to the particle size, which influences bioavailability and circulation time, the wide-area by volume ratio (increased solubility compared to larger particles). Such properties make ideal nanoparticulate candidates for investigation and enhancement of therapeutic impacts (Al Musawi *et al.* 2020; Haider *et al.* 2021). Al_2O_3-NPs are a class of metal oxide NPs with varied biomedical applications due to their unique physicochemical and structural characteristics (Xiang *et al.* 2011). By conjugating chosen ligands, proteins, antibodies, medicines, and enzymes to Al_2O_3-NPs, they may be tailored to the particular binding behaviour of selected target cells, increasing their targeted drug delivery capacity and therapeutic effectiveness at the disease site (Lu *et al.* 2008). This study aimed to develop methods for developing Al_2O_3-NPs and evaluate them as antiviral therapy against pathogenic HSV-1 infection.

MATERIALS AND METHODS

Materials

Al_2O_3-NPs (powder form) were obtained from Merck Company (Germany; Catalogue Number: 108846). NPs were suspended in Dulbecco's Modified Eagle's medium (DMEM; Co., Ltd., Shangdong, Yantai, China) to allow various concentrations. NPs suspension was subjected to sonication to reduce aggregation. Acyclovir agent was obtained from Sigma-Aldrich (Shanghai, China), dissolved in DMEM, and utilized in various concentrations as a typical agent for HSV-1 treatment.

Characterization of nanoparticles

FESEM (Hitachi S-4160, Japan), HRTEM (Carl Zeiss AG-Zeiss EM900, Germany), DLS (Malvern Instruments Ltd., Malvern, UK), and XRD (SIEMENS-D5000) analyses were utilized to achieve morphological, dimensional, structural, and scale data on NPs.

Cell and virus culture

Fibroblast cells were provided from the American Type Culture Collection (ATCC). DMEM with 10% foetal bovine serum and 100 g mL^{-1} streptomycin were used to culture fibroblast cells, 2 mM L-glutamine, 1 mM sodium pyruvate and 100 IU mL^{-1} penicillin (Sigma-Aldrich, USA). The cells were grown at 37 °C in a humidified incubator with a 5% CO_2 environment. The vaccine and sera institute provided the HSV-1 stock (Baghdad, Iraq). HSV-1 was propagated in fibroblast cells, titrated using the Reed and Muench formula for 50% tissue culture infectious dose ($TCID_{50}$), and preserved in sterile cryovials at 80 °C.

MTT assay

The methyl thiazolyl tetrazolium (MTT) test was used to assess the impact of Al_2O_3-NPs on fibroblast cell survival. In a 96-well flat-bottomed microtiter plate (Nalge Nunc, Naperville, IL), fibroblast cells (1×10^5 cells mL^{-1}) were sown and cultured for 24 h at 37 ° C. In triplicate, different Al_2O_3-NP concentrations (20 to 140 g mL^{-1}) were applied to the plate. A volume of 5 µL of MTT powder (5 mg mL^{-1}; Roche, Mannheim, Germany) was applied to each well after 48 h of incubation at 37 ° C, and the plate was incubated in the dark at 37 ° C for 3 h. The MTT solution was then discarded, followed by adding 50 µL tidy dimethyl sulfoxide (Sigma-Aldrich, USA) to each well, and the plate was gently shaken for 10 min at ambient temperature. Afterward, the plate reading was performed at 550 nm in a microplate reader (Synergy 4, Biotek Instruments, Winooski, VT, USA), and the cell viability ratio was measured for each dose, compared to untreated control cells.

Determination of antiviral activity

In a humidified environment comprising 5% CO_2, confluent monolayers of fibroblast cells in a flat-bottomed 96-well microtiter plate were treated with 100 L of 100 $TCID_{50}$ mL^{-1} HSV-1 for 1 h at 37 °C. After removing the viral inocula, the monolayers were rinsed triplicate with papered PBS to eliminate any remaining viruses. The infected cells were subsequently cultured for 48 h at 37 °C in a humidified 5 percent CO_2 environment with 100 L of various non-cytotoxic doses of Al_2O_3-NPs. This experiment also contained a cell control (uninfected cells in DMEM) and a viral control (virus + DMEM). Acyclovir was also tested using this method. Following the

incubation period, the cells were frozen and thawed once again to liberate the cell-related virus bodies. Subsequently, the lysates from the wells were utilized in q RT-PCR and $TCID_{50}$ experiments.

Quantitative RT-PCR

The Genomic DNA Isolation Mini Kit was used to extract HSV-1 DNA from the collected lysate according to the manufacturer's instructions (Qiagen, UK). The primers 5′-TGA GGC GCG ATT CTG GATGC-3′ and 5′-AAC GCG TCC TTG TTC TCG GC-3′were used to amplify the US3 region 127-bp fragment in a quantitative RT-PCR. The reaction condition settings for RT-PCR were the same as in the previous work (Abdul Mahdi *et al.* 2021). RT-PCR was carried out by means of Rotor-Gene Q equipment (Qiagen, UK). As a template, a recombinant plasmid carrying a 127-bp DNA fragment of the HSV-1 US3 gene was utilized. The segment was cloned onto the pGH plasmid vector, and delivered as a lyophilized powder. The preparation of recombinant plasmid and cloning process were handled by Generay Biotech (Shanghai, China). To make a stock solution, 4 g of the template was weighed and dissolved in 40 L of dilution buffer to get a 100 ng mL^{-1} solution. After measuring the template DNA concentration by means of a NanoDrop spectrophotometer, the DNA template copy number in the standard stock was measured utilizing the Sequencing Center & URI Genomics software (Thermo Fisher Scientific, Grand Island, NY, USA). The serially dilution performed for stock solution was ten times and used as a template to generate standard curves. The HSV-1 copy number in the unknown samples was determined using the standards.

Indirect immunofluorescence assay (IFA)

A 24-well tissue culture plate was utilized for fibroblast cells seeding and culturing in the wells using sterilized glass coverslips (Sigma-Aldrich, USA; Qiagen, UK). After attainment 85% confluency, the medium was withdrawn, and the cells were subjected to a humidified environment at 37 ºC with 5% CO_2 for 1 h with 200 L of 100 $TCID_{50}$ mL^{-1} HSV-1 solution. The viral inocula were then withdrawn, and the plate was incubated at 37 °C with the highest non-cytotoxic concentration of ZnO-NPs. This experiment also contained a cell control (treated uninfected cells) and a viral control (untreated infected cells). The cells were fixed with cold acetone for 15 min after 14 h of treatment, then treated with HSV-1 specific human antibody for 45 min at room temperature. After three washes with PBS, the cells were treated for 40 min at room temperature with goat anti-human IgG conjugated with fluorescein isothiocyanate (FITC; Sigma-Aldrich, USA). The labelled cells were rinsed three times in PBS before being examined with an Olympus BH2-RFCA fluorescence microscope (Tokyo, Japan).

Statistical analysis

GraphPad Prism software (ver. 9.0) was applied to conduct statistical analyses, which included one-way analysis of variance (ANOVA) and Tukey's multiple comparison test. The error bars show the standard deviation, and the results represent the mean of three separate experiments. Statistical significance was determined by p-values less than 0.05.

RESULTS

Characterization

DLS-determined Al_2O_3-NPs were found 120.8 ± 21.7 nm with 0.126 ± 0.05 mV polydispersity index (PDI; Fig. 1A). As shown in Fig. 1B, the crystal structure of Al_2O_3-NPs was studied using XRD. All nine diffraction peaks' position and relative strength corresponded well to the Normal Al_2O_3-NPs XRD sequence, comparable with the spectra previously mentioned (Fig. 1B; Gaikwad et al. 2013; Sezer *et al.* 2018). Morphology of Al_2O_3-NPs and their size were characterized using FESEM and DLS techniques. FESEM images showed spherically distributed Al_2O_3-NPs with identical particle shape and size distribution and 120 nm mean diameter (Figs. 2A - B).

MTT results

The MTT test was used to assess the cytotoxicity of Al_2O_3-NPs on fibroblast cells (Fig. 3) demonstrating the viability of fibroblast cells subjected to Al_2O_3-NPs at concentrations of 20, 40, 60, 80, 100, and 120 µg mL^{-1} ($p = 0.0001$). Three separate experiments' mean values are shown by vertical lines. When the quantity of Al_2O_3-NPs was raised to 120 µg mL^{-1}, the cell viability dropped to 48.32% compared to control cells. Antiviral tests were conducted using different concentrations of Al_2O_3-NPs that exhibited a cytotoxic impact of less than 10%.

Cytopathic effects (CPE)

In the presence of Al_2O_3-NPs, cytotoxic effects on fibroblast cells infected by HSV-1 were observed. The result indicated a reduced CPE caused by HSV-1 in Al_2O_3-NPs-untreated and treated HSV-1-infected Vero cells using an inverted microscope in a dose-dependent manner (Nikon, Japan).

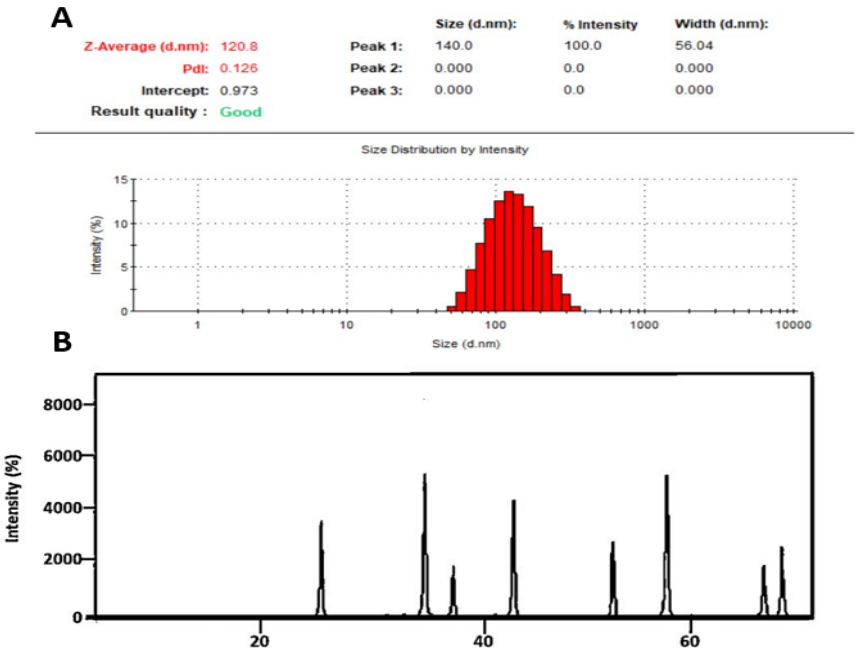

Fig. 1. Size measurement images. The Al_2O_3-NPs size using dynamic light scattering (DLS) (A) and crystal structure of the Al_2O_3-NPs with XRD (B).

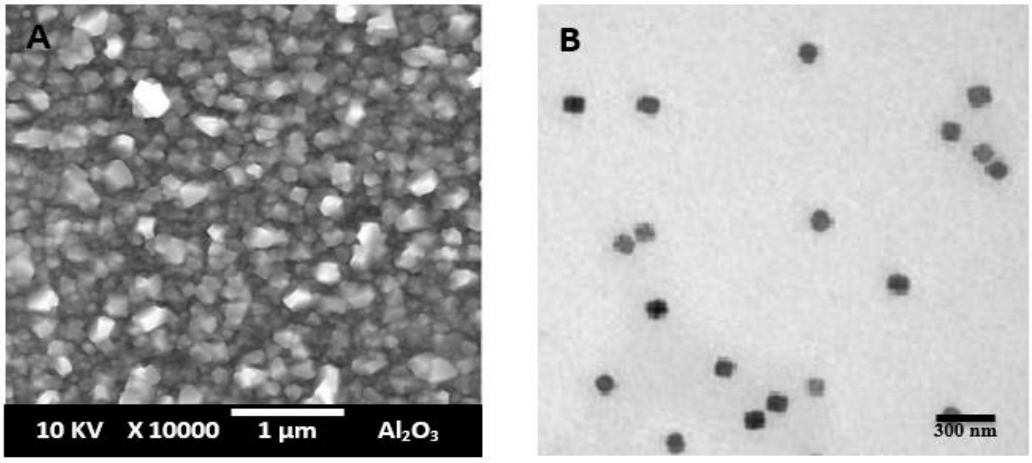

Fig. 2. FESEM image of Al_2O_3-NPs (magnification 10 kX) (C); TEM image of Al_2O_3-NPs (D).

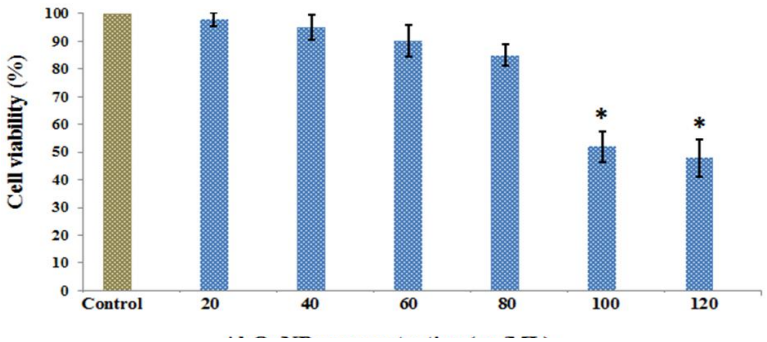

Fig. 3. Cytotoxic study of Al_2O_3-NPs on fibroblast cells utilizing the MTT test.

At a dosage of 100 µg mL^{-1}, HSV-1-infected cells were treated with Al_2O_3-NPs. HSV-1 caused significant cytopathic effects in fibroblast cell monolayers 48 h after viral injection (Fig. 4). These effects included cell rounding, refringence, and syncytia formation. In Al_2O_3-NPs-treated fibroblast cells infected with HSV-1, cytotoxic effects were decreased. The maximum utilized concentration (100 µg ml^{-1}) of Al_2O_3-NP was linked to a roughly 10% cytotoxic impact on the fibroblast cells. As a result, the shape of certain cells was changed in comparison with the control, unrelated to HSV-1-stimulated cytopathic consequences (Fig. 4).

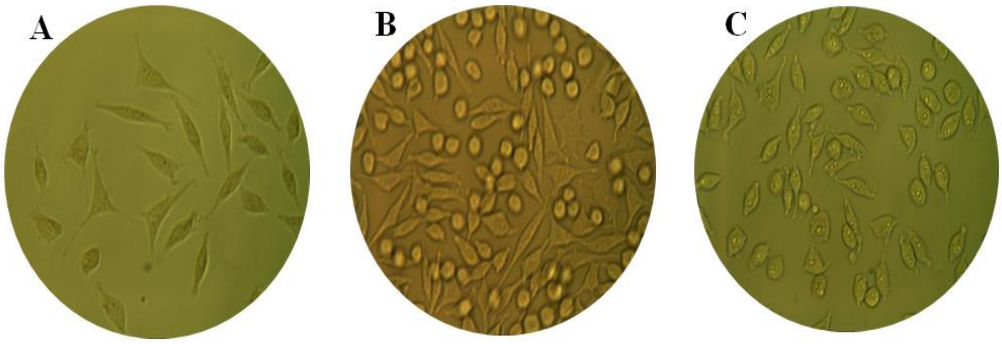

Fig. 4. Prevention of cytopathic effects of HSV-1 on fibroblast cells once using Al_2O_3-NPs treatment (A) cell control (B) and virus control (C).

Evaluation of antiviral activity

The $TCID_{50}$ test was used to evaluate the viability of fibroblast cells and the antiviral efficacy of Al_2O_3-NPs on the infected titer of HSV-1. Al_2O_3-NPs exhibited a substantial inhibitory impact on HSV-1 activity at a concentration of 100 µg mL^{-1}. When HSV-1 infected cells were exposed to 20, 40, 80, and 100 µg mL^{-1} Al_2O_3-NPs, the infected titer of HSV-1 was reduced using 0.1, 0.7, 1.8, and 2.5 log_{10} $TCID_{50}$, respectively, compared to viral control (p-value = 0.0001; Fig. 5).

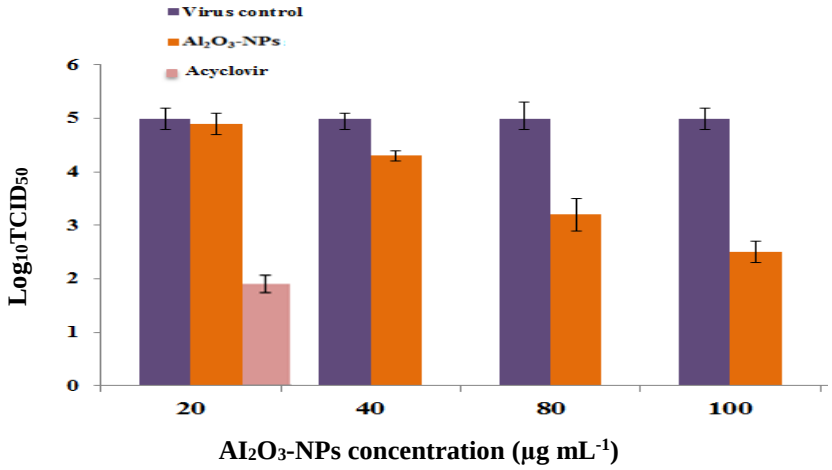

Fig. 5. Comparison of antiviral effect of Al_2O_3-NPs and acyclovir on the infected titer of HSV-1 using the $TCID_{50}$ test. When HSV-1 infected cells were exposed to 20, 40, 80, and 100 g/mL Al_2O_3-NPs, the infected titer of HSV-1 was reduced by 0.1, 0.7, 1.8, and 2.5 log_{10} $TCID_{50}$, respectively, compared to viral control.

Real-Time PCR

Real-time PCR was used to study the activity of Al_2O_3-NPs on HSV-1 viral load, which was established on the multiplication of a 127-bp segment from a exceedingly preserved location of the HSV-1 US3 gene by means of SYBR Green q RT-PCR Master Mix. The activity of Al_2O_3-NPs on HSV-1 virus as specified using real-time PCR is shown in Fig. 6. The inhibition rates of Al_2O_3-NPs at different concentrations (20, 40, 60, 80, and 100 µg mL^{-1}) were 16.9%, 47.1%, 61.2%, 72.5%, and 74.6 %, respectively, depending on the HSV-1 viral load (Fig. 6). At a dose of 40 µg mL^{-1}, acyclovir showed full suppression of the HSV-1 infectious titer and a 100% inhibition rate (p = 0.0001).

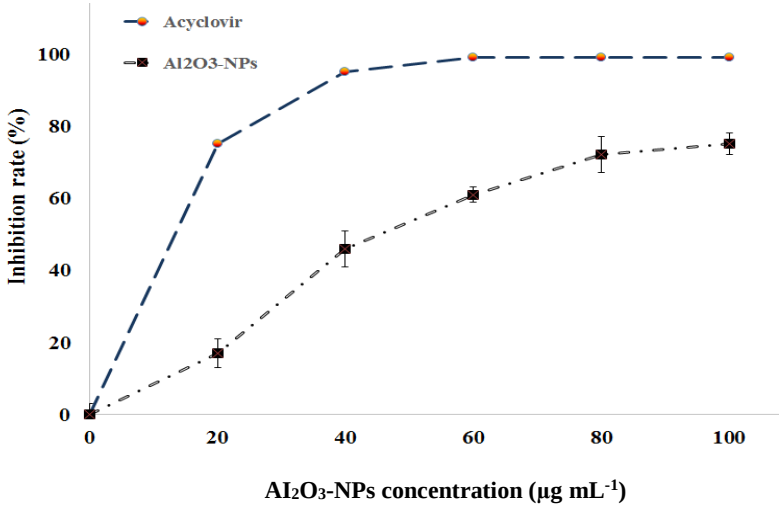

Fig. 6. Real-time PCR analysis of the effect of Al_2O_3-NPs on HSV-1 viral load. The inhibition rates of Al_2O_3-NPs at doses of 20, 40, 60, 80, and 100 µg mL^{-1} were 16.9%, 47.1%, 61.2%, 72.5%, and 74.6%, respectively, depending on the HSV-1 viral load.

IFA results

In this experiment, we assessed the consequence of Al_2O_3-NPs treatment on HSV-1 antigen expression in fibroblast cells by an immunofluorescence test (IFA). In an IFA research, Al_2O_3-NPs were found to exhibit inhibitory effects on the HSV-1 antigens expression on the fibroblast cells surface. According to virus control, cell control, and HSV-1 infected cells, the cells were treated with 100 µg mL^{-1} Al_2O_3-NPs. When HSV-1 infected cells were treated with Al_2O_3-NPs, the intensity of fluorescence signals was noticeably reduced compared to virus control, confirming that Al_2O_3-NPs had a potent antiviral impact on HSV-1 antigen expression (Fig. 7).

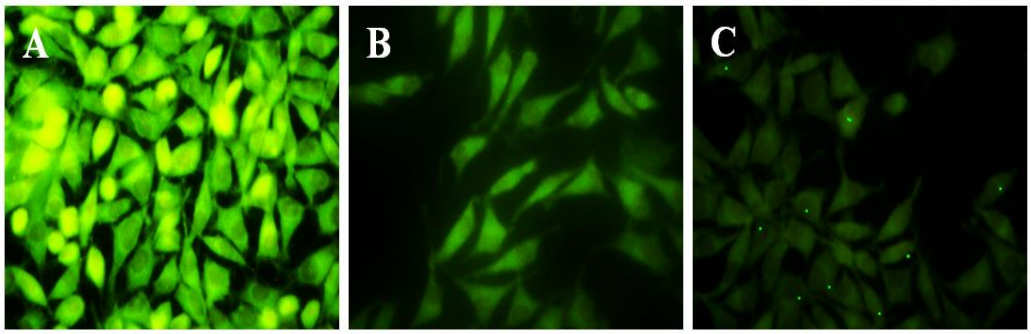

Fig. 7. The impact of Al_2O_3-NPs on the HSV-1 antigens expression of fibroblast cells was assessed using an immunofluorescence test (IFA). HSV-1 infected cells treated with 100 µg mL^{-1} Al_2O_3-NPs. (A) Virus control, (B) Cell control, (C) HSV-1 infected cells treated with 100 µg mL^{-1} Al_2O_3-NPs. When HSV-1 infected cells were treated with Al_2O_3-NPs, the intensity of fluorescence signals was substantially reduced compared to the virus control, suggesting that Al_2O_3-NPs had a strong antiviral effect on HSV-1 antigen expression. The green spots in Fig. 7C represent expression level of viral antigens in various cell section and were discoloured with goat anti-human IgG coupled with FITC.

DISCUSSION

NPs have been widely studied for use as medication carriers and antibacterial agents in a variety of areas (Al-Kinani *et al.* 2020; Al Musawi *et al.* 2021). Aside from that, NPs exhibit broad antiviral efficacy due to their multi-targeting chemical processes. Viruses such as the human immunodeficiency virus, hepatitis B virus, and herpes simplex virus have been found to be resistant to silver NPs (Mukherjee *et al.* 2011; Maruzuru *et al.* 2014). Aluminium is an all-encompassing metal element especially suited for various applications in biomedicine (Ziuba *et al.* 2012). In recent years, NPs of aluminium oxide and their compounds have been identified as active agents for various pathogens (Zhang *et al.* 2017). Due to extremely limited studies in this regard, it is important to study

the inhibitory capacity of Al_2O_3-NPs for viral infection, especially against HSV-1. Based on the findings, Al_2O_3-NPs may be a new antiviral component for HCV-1 treatment. Within the culture system of fibroblast cells, the Al_2O_3-NPs were shown to substantially suppress HSV-1 infection. In the present study, many laboratory techniques, including $TCID_{50}$, Real-Time PCR, and IFA assays, verified the suppression of viral infection. Our aim was to evaluate the antiviral effectiveness of Al_2O_3-NPs that were injected into the cell following HSV-1 adsorption. Once HSV-1 infects a cell, it transports the nucleocapsid from the cytosol to the nucleus via nuclear membrane pores. All processes of viruses such as capsid development, gene replication, expression, and their DNA packing take place in the nucleus area of infected cells (Alexis *et al.* 2020). In one or more of those phases of viral replication, Al_2O_3-NPs may be interfering factors. (Francisco *et al.* 2018). Aluminium ions released from Al_2O_3-NPs were found to affect various targets directly and result in ROS development, resulting in DNA denaturation and cell integrity damage (Caitlin *et al.* 2021). We hypothesize that these action mechanisms can also help against viral infections.

CONCLUSION

In summary, Al_2O_3-NPs have considerable antiviral efficacy against HSV-1, according to our findings. Antiviral behaviour of Al_2O_3-NPs, is thought to be explained by a variety of mechanisms such as the production of reactive oxygen species by free Al ions from NPs, which may contribute to HSV-1 inactivation through viral protein oxidation or viral genome destruction.

ACKNOWLEDGMENTS

The authors appreciate Al-Qasim Green University for their technical support. Author contributions Conceptualisation: S.A.-M, A. K. A, and H. A., Methodology: S.A.-M, A. K. A, Validation: S.A.-M, A. K. A, B. B, Formal Analysis: B. B, Investigation: S.A.-M, A. K. A., Resources: S.A.-M, A. K. A, H. ., B. B., Writing–Original Draft Preparation: S.A.-M, A. K. A., Writing – Review and Editing: S.A.-M., Supervision: S.A.-M, A. K. A.,

Conflicts of Interest: The authors declare no conflict of interest.

REFERENCES

Abdul Mahdi, S, Kadhim, AA, Albukhaty, S, Nikzad, S, Haider, AJ, Ibraheem, S, Kadhim, HA & Al Musawi S 2021, Gene expression and apoptosis response in hepatocellular carcinoma cells induced by biocompatible polymer / magnetic nanoparticles containing 5-Fluorouracil. *Electronic Journal of Biotechnology*, 52: 21–28. DOI:10.1016/j.ejbt.2021.04.001.

Al Awady, MJ, Balaki,t AA, Al Musawi, S, Alsultani, MJ, Kamil, A & Alabbasi M, Investigation of Anti-MRSA and Anticancer Activity of Eco-Friendly Synthesized Silver Nanoparticles from Palm Dates Extract. *Nano Biomedicine and Engineering*, 11:157-169.

Albukhaty, S, Al Bayati, L, Al Karagoly, H & Al Musawi, S 2020, Preparation and characterization of titanium dioxide nanoparticles and in vitro investigation of their cytotoxicity and antibacterial activity against Staphylococcus aureus and Escherichia coli. *Animal Biotechnology*, 28:1-7. DOI: 10.1080/10495398.2020.1842751.

Albukhaty, S, Al Musawi, S, Abdul Mahdi, S, Sulaiman, GM, Alwahibi, MS, Dewir, YH, Soliman, DA & Rizwana, H 2020, Investigation of Dextran-Coated Superparamagnetic Nanoparticles for Targeted Vinblastine Controlled Release, Delivery, Apoptosis Induction, and Gene Expression in Pancreatic Cancer Cells. *Molecules*, 25: 4721. DOI: 10.3390/molecules25204721.

Al Kaabi, WJ, Albukhaty, S, Al Fartosy, AJM. Al Karagoly, HK, Al Musawi, SM, Sulaiman, GM, Dewir, YH, Alwahibi, MS & Soliman, DA 2021, Development of *Inula graveolens* (L.) Plant Extract Electrospun/Polycaprolactone Nanofibers: A Novel Material for Biomedical Application. *Applied Sciences*, 11: 828, DOI: 10.3390/app11020828.

Al Kinani, MA, Haider, AJ & Al Musawi, S 2021, Design and synthesis of nanoencapsulation with a new formulation of Fe@Au-CS-CU-FA NPs by Pulsed Laser Ablation in Liquid (PLAL) method in breast cancer therapy: *In vitro* and *in vivo*. *Plasmonics*, DOI: 10.1007/s11468-021-01371-3.

Al Kinani, MA, Haider, AJ & Al Musawi, S 2020, Design, construction and characterization of intelligence polymer coated core–shell nanocarrier for curcumin drug encapsulation and delivery in lung cancer therapy purposes. *Journal of Inorganic and Organometallic Polymers and Materials*.

Al Kinani, MA, Haider, AJ & Al Musawi, S 2020, High uniformity distribution of fe@au preparation by a micro-emulsion method. IOP Conference Series: Materials Science and Engineering. Eng. 987: 012013, DOI:10.1088/1757-899X/987/1/012013.

Al Musawi, S, Hadi, AJ, Hadi, SJ & Hindi, NKK 2019, Preparation and characterization of folated chitosan-magnetic nanocarrier for 5-fluorouracil drug delivery and studying its effect in bladder cancer therapy. *Journal of Global Pharma Technology*, 11: 628-637.

Al Musawi, S, Hadi, AJ, Hadi, SJ & Hindi, NKK 2019, Preparation and characterization of folated chitosan-magnetic nanocarrier for 5-fluorouracil drug delivery and studying its effect in bladder cancer therapy. *Journal of Global Pharma Technology*, 11:628-637.

Al Musawi, S, Kadhim, MJ & Hindi, NKK 2018, Folated-nanocarrier for paclitaxel drug delivery in leukemia cancer therapy. *Journal of Pharmaceutical Sciences and Research*, 10: 749-754.

Al Musawi, S, Albukhaty, S, Al Karagoly, H & Almalki, F 2020, Design, and synthesis of multi-functional superparamagnetic core-gold shell coated with chitosan and folate nanoparticles for targeted antitumor therapy. *Nanomaterials*, 11: 1, DOI: 10.3390/nano11010032.

Al Musawi, S, Albukhaty, S, Al Karagoly, H, Sulaiman, GM, Alwahibi, MS, Dewir, YH, Soliman, DA & Rizwana, H 2020, Antibacterial activity of honey/chitosan nanofibers loaded with capsaicin and gold nanoparticles for wound dressing. *Molecules*, 25: 4770, DOI: 10.3390/molecules25204770.

Al Musawi, S, Ibraheem, S, Mahdi, SA, Albukhaty, S, Haider, AJ, Kadhim, AA, Kadhim, KA, Kadhim, HA & Al Karagoly, H 2021, Smart nanoformulation based on polymeric magnetic nanoparticles and vincristine drug: a novel therapy for apoptotic gene expression in tumour. *Life*, 11: 71. DOI: 10.3390/life 11010071.

Al Musawi, S, Albukhaty, S, Al Karagoly, H, Sulaiman, GM, Jabir MS & Naderi Manesh, H 2020, dextran-coated superparamagnetic nanoparticles modified with folate for targeted drug delivery of camptothecin. *Advances in Natural Sciences: Nanoscience and Nanotechnology*, 11: 045009. DOI: 10.1088/2043-6254/abc75b.

Carmody, CM, Goddard, JM & Nugen, SR 2021, Bacteriophage capsid modification by genetic and chemical methods. *Bioconjugate Chemistry*, 32:466-481. 10.1021/acs.bioconjchem.1c00018.

Duarte, LF, Farías, MA, Álvarez, DM, Bueno, SM, Riedel, CA & González, PA 2019, Herpes simplex virus type 1 infection of the central nervous system: insights into proposed interrelationships with neurodegenerative disorders. *Frontiers in Cellular Neuroscience*, 13: 46.

Falih, BT, Mohammed, ST & Mohammed, NJ 2022, Effects of the silver nanoparticle synthesis from the leaves of the *Capparis spinosa* plant on the liver of mice infected with visceral leishmaniasis. *Caspian Journal of Environmental Sciences*, 20: 785-791.

Gaikwad, S, Ingle, A, Gade, A *et al.* 2013, Antiviral activity of mycosynthesized silver nanoparticles against herpes simplex virus and human parainfluenza virus type 3. *International Journal of Nanomedicine*, 8: 4303-4314, DOI:10.2147/IJN.S50070

Haider, AJ, Al Kinani, MA & Al Musawi, S 2021, Preparation and characterization of gold coated super paramagnetic iron nanoparticle using pulsed laser ablation in liquid method. *Key Engineering Materials*, 886: 77-85. DOI:10.4028/www.scientific.net/KEM.886.77.

Haider, AA & Hussein, HZ 2022, Efficiency of biologically and locally manufactured silver nanoparticles from *Aspergillus niger* in preventing *Aspergillus flavus* to produce aflatoxin B1 on the stored maize grains. *Caspian Journal of Environmental Sciences*, 20: 765-773.

Huet, A, Huffman, JB, Conway, JF & Homa, FL 2020, Role of the herpes simplex virus CVSC proteins at the capsid portal vertex. *Journal of Virology*, 94: 24.10.1128/JVI.01534-20.

Ibáñez, FJ, Farías, MA, Gonzalez Troncoso, MP, Corrales, N, Duarte, LF, Díaz, AR & González, PA 2018, Experimental dissection of the lytic replication cycles of herpes simplex viruses in vitro. *Frontiers in Microbiology*, 9, 10.3389/fmicb.2018.02406.

James, SH, Sheffield, JS & Kimberlin, DW 2014, Mother to child transmission of herpes simplex virus. *Journal of the Pediatric Infectious Diseases Society*, 3: S19-S23. DOI:10.1093/jpids/piu050.

Kakiuchi, S, Tsuji, M, Nishimura, H *et al.* 2017, Association of the emergence of acyclovir-resistant herpes simplex virus type 1 with prognosis in hematopoietic stem cell transplantation patients. *The Journal of Infectious Diseases*, 215: 865-873.

Kongyingyoes, B, Priengprom, T, Pientong, C, Aromdee, C, Suebsasana, S & Ekalaksananan T 2016, isopropylidene andrographolide suppresses early gene expression of drug-resistant and wild type herpes simplex viruses. *Antiviral Research*, 3: 132:281-286.

Lu, L, Sun, RW, Chen, R *et al.* 2008, Silver nanoparticles inhibit hepatitis B virus replication. *Antiviral Therapy*, 13:253-262.

Maruzuru, Y, Shindo, K, Liu, Z, Oyama, M, Kozuka Hata, H, Arii, J *et al.* 2014, Role of herpes simplex virus 1 immediate early protein ICP22 in viral nuclear egress. *Journal of Virology*, 88: 7445-7454.

Morfin, F & Thouvenot D 2003, Herpes simplex virus resistance to antiviral drugs. *Journal of Clinical Virology*, 26: 29-37.

Mukherjee, A, Mohammed Sadiq, I, Prathna, TC & Chandrasekaran, N 2011, Antimicrobial activity of aluminium oxide nanoparticles for potential clinical applications. *Science and Technology Against Microbial Pathogens Communication Research Advanced Materials Technologies*, 1: 245-251.

Priengprom, T, Ekalaksananan, T, Kongyingyoes, B, Suebsasana, S, Aromdee, C & Pientong, C 2015, Synergistic effects of acyclovir and 3, 19-isopropylideneandrographolide on herpes simplex virus wild types and drug-resistant strains. *BMC Complementary Medicine and Therapies*, 15:56.

Sezer, NZ, Evis, SM, Kayhan, A, Tahmasebifar, M 2018, Koç review of magnesium-based biomaterials and their applications. *Journal of Magnesium and Alloys*, 6: 23-43.

Suhad, H, Neihaya, HZ, Raghad, AL 2021, Evaluating the biological activities of biosynthesized ZnO nanoparticles using *Escherichia coli*. *Caspian Journal of Environmental Sciences*, 19: 809-815

Trigilio, J, Antoine, TE, Paulowicz, I, Mishra, YK, Adelung, R & Shukla, D 2012, Tin oxide nanowires suppress herpes simplex virus-1 entry and cell-to-cell membrane fusion. *PLoS ONE*, 7: e48147.

Xiang, DX, Chen, Q, Pang, L, Zheng, CL 2011, Inhibitory effects of silver nanoparticles on H1N1 influenza: A virus *in vitro*. *Journal of Virological Methods*, 178:137-142. DOI: 10.1016/j.jviromet.2011.09.003

Zhang, J, Liu, H & Wei, B 2017, Immune response of T cells during herpes simplex virus type 1 (HSV-1) infection. *Journal of Zhejiang University-Science B*, 18: 277-288. DOI:10.1631/jzus. B1600460.

Zhang, Q, Wang, H, Ge, C, Duncan, J, He, K, Adeosun, SO *et al.* 2017, Alumina at 50 and 13 nm nanoparticle sizes have potential genotoxicity. *Journal of Applied Toxicology*, 9:1053-64.

Ziuba, N, Ferguson, MR, O'Brien, WA *et al.* 2012, Identification of cellular proteins required for replication of human immunodeficiency virus type 1. *AIDS Research and Human Retroviruses*, 28: 1329-1339.

Bibliographic information of this paper for citing:

Almansorri, AK, Al-Shirifi, HMH, Al-Musawi, S & B Ahmed, B 2023. Inhibition activity of aluminium oxide nanoparticles for herpes simplex type 1. Caspian Journal of Environmental Sciences, 21: 125-133.